

Sodium Dependent Taurine Transport into the Choroid Plexus, the Blood-Cerebrospinal Fluid Barrier

Suk-Jae Chung^{1†}, Vikram Ramanathan², Claire M. Brett
and Kathleen M. Giacomini²

¹Department of Pharmaceutics, College of Pharmacy, Seoul National University

²Department of Pharmacy and Anesthesia, University of California at San Francisco

(Received April 21, 1995)

Taurine, a β -amino acid, plays an important role as a neuromodulator and is necessary for the normal development of the brain. Since *de novo* synthesis of taurine in the brain is minimal and *in vivo* studies suggest that taurine does not cross the blood-brain barrier, we examined whether the choroid plexus, the blood-cerebrospinal fluid (CSF) barrier, plays a role in taurine transport in the central nervous system. The uptake of [³H]-taurine into ATP depleted choroid plexus from rabbit was substantially greater in the presence of an inwardly directed Na⁺ gradient taurine accumulation was negligible. A transient in side-negative potential gradient enhanced the Na⁺-driven uptake of taurine into the tissue slices, suggesting that the transport process is electrogenic. Na⁺-driven taurine uptake was saturable with an estimated V_{max} of 111 ± 20.2 nmole/g/15 min and a K_M of 99.8 ± 29.9 μ M. The estimated coupling ratio of Na⁺ and taurine was 1.80 ± 0.122 . Na⁺-dependent taurine uptake was significantly inhibited by β -amino acids, but not by α -amino acids, indicating that the transporter is selective for β -amino acids. Since it is known that the physiological concentration of taurine in the CSF is lower than that in the plasma, the active transport system we characterized may face the brush border (*i.e.*, CSF facing) side of the choroid plexus and actively transport taurine out of the CSF. Therefore, we examined *in vivo* elimination of taurine from the CSF in the rat to determine whether elimination kinetics of taurine from the CSF is consistent with the *in vitro* study. Using a stereotaxic device, cannulae were placed into the lateral ventricle and the cisterna magna of the rat. Radio-labelled taurine and inulin (a marker of CSF flow) were injected into the lateral ventricle, and the concentrations of the labelled compounds in the CSF were monitored for upto 3 hrs in the cisterna magna. The apparent clearance of taurine from CSF was greater than the estimated CSF flow ($p < 0.005$) indicating that there is a clearance process in addition to the CSF flow. Taurine distribution into the choroid plexus was at least 10 fold higher than that found in other brain areas (*e.g.*, cerebellum, olfactory bulb and cortex). When unlabelled taurine was co-administered with radio-labelled taurine, the apparent clearance of taurine was reduced ($p < 0.01$), suggesting a saturable disposition of taurine from CSF. Distribution of taurine into the choroid plexus, cerebellum, olfactory bulb and cortex was similarly diminished, indicating that the saturable uptake of taurine into these tissues is responsible for the non-linear disposition. A pharmacokinetic model involving first order elimination and saturable distribution described these data adequately. The Michaelis-Menten rate constant estimated from *in vivo* elimination study is similar to that obtained in the *in vitro* uptake experiment. Collectively, our results demonstrate that taurine is transported in the choroid plexus via a Na⁺-dependent, saturable and apparently β -amino acid selective mechanism. This process may be functionally relevant to taurine homeostasis in the brain.

Taurine, a β -amino acid, is essential for normal development and function of the cerebellum and visual cortex, as well as the retina.¹⁻⁴⁾ Also, tau-

rine has been shown to alter the release of neurotransmitters such as acetylcholine and norepinephrine,⁵⁾ and, thus, it is generally accepted to

[†] To whom correspondence should be addressed.

be a neuromodulator.^{5, 6)}

Biosynthesis of taurine is minimal in brain^{6, 7)} so that a systemic source is essential. Since taurine is zwitterionic at physiologic pH, it is unlikely that taurine diffuses passively through biological membranes. Therefore, its transport into or out of the brain must involve carrier-mediated process(es) at the blood-brain barrier and/or the blood-cerebrospinal fluid (CSF) barrier. In general, such membrane-associated transport system(s) at the barriers of the central nervous system (CNS) functions to provide a protected environment for the brain by selectively excreting certain substances and reabsorbing others. However, the site and underlying mechanism for taurine's entry into or exit from the CNS is currently unknown.

Recently, Na⁺-dependent taurine transporter has been cloned from the human thyroid,⁸⁾ the human placenta⁹⁾ and the mouse brain.¹⁰⁾ Interestingly, Liu *et al.*¹⁰⁾ reported that the brain microvessel, the blood brain barrier, did not contain mRNA for the taurine transporter. This observation suggests that the blood-CSF barrier, rather than the blood-brain barrier, may be an important site for maintaining homeostasis of taurine in the brain.

Although few data are available specifically for taurine, an important role for the choroid plexus in maintaining homeostasis of α -amino acids in the brain has been suggested by both *in vitro*^{11, 12)} and *in vivo*^{13, 14)} studies. For example, it has been documented that isolated choroid plexus tissue slices accumulate α -amino acids against a concentration gradient via saturable and energy dependent mechanism.^{11, 12)} Also, in the perfused choroid plexus of the sheep, Preston and Segal noted that the net flux for several α -amino acids between blood and the CSF could be directed into or out of the CSF depending on the amino acid concentrations in the biological fluids.¹³⁾ These observations suggest that the choroid plexus plays a significant role in regulating the concentrations

of α -amino acids in the CSF and in maintaining the low CSF to plasma concentration ratios.^{15, 16)} However, there are no available data in the literature to explain the low CSF to plasma ratio of taurine.

Based on the recent biochemical evidence that reports the absence of a taurine transporter in the blood-brain barrier, we hypothesized that the choroid plexus is a site for the transport of taurine via the CSF. Thus, the objectives of this study were to determine whether taurine is transported in the choroid plexus and to characterize the mechanism responsible for its transport. In addition, we were interested in comparing *in vitro* uptake kinetics and *in vivo* elimination characteristics of taurine. We describe a Na⁺-dependent transport system for taurine in choroid plexus. Kinetics of elimination for taurine *in vivo* was also similar to that found in the *in vitro* uptake experiment. These observations suggest that the taurine transporter in the choroid plexus is important in maintaining homeostasis of taurine in the CSF and, ultimately, the extracellular fluid of the brain.

Materials and Methods

Materials

[³H] Taurine (21.9 Ci/mmol) and [¹⁴C] inulin (2.8 mCi/g) was obtained from Du Pont-New England Nuclear (Boston, MA). [¹⁴C] Mannitol was obtained from Moravек Biochemicals (Brea, CA). All other chemicals were purchased from Sigma Chemical Co. (St. Louis, MO). New Zealand White rabbits were purchased from Nitabell Rabbitry (Hayward, CA). Male Sprague-Dawley rats (270~300 g) were purchased from Simonson Inc. (Gilroy, CA). Cytocint ES scintillation fluid was obtained from ICN Biomedical Inc. (Irvine, CA). Acepromazine was obtained from Aveco Co., Inc. (Fort Dodge, Iowa). Ketamine was obtained from Fort Dodge Laboratories, Inc. (Fort Dodge, Iowa).

Preparation of ATP-depleted Choroid Plexus

Choroid plexus was obtained from male New Zealand White rabbits (2~3 kg) and ATP-depleted by the method of Carter-Su and Kimmich,¹⁷ modified by Suzuki *et al.*¹⁸ and our laboratory.¹⁹ Briefly, rabbits were anesthetized with ketamine (5 mg/kg) and then quickly decapitated. The choroid plexuses were immediately isolated from the lateral ventricles and placed in either of the following buffers (mM) : KCl(120), mannitol (40), HEPES (25), or NaCl (120), mannitol (40), HEPES (25), pH 7.4 with 1 M Tris. The choroid plexuses were cut into 2~3 mm pieces and then placed into buffer containing 250 μ M 2,4-dinitrophenol (DNP) for 20 min at 37°C to deplete the tissue of ATP. When it was necessary to prevent the development of an electrical potential gradient, the tissue slices were initially equilibrated in either (mM) choline chloride (120), KCl (40), HEPES (15) (pH 7.4, adjusted with 1 M Tris) or NaCl (120), KCl(40), HEPES (15) (pH 7.4, adjusted with 1 M Tris) and the K⁺ ionophore, valinomycin (10 μ M), was added along with DNP.

In all studies, after ATP-depletion, the tissue slices were stored in buffer on ice, until the experiments were performed (<2 hrs after the DNP treatment). For the initiation of uptake, the tissue slices were removed from the preloading buffer, blotted lightly on a tissue paper and added to the appropriate reaction mixture (see Uptake Studies).

Electrical Potential Gradient Studies

To test whether Na⁺-dependent taurine uptake is electrogenic, the Na⁺-dependent taurine uptake in the presence of inside negative potential gradient was compared to that under voltage clamped condition. In these studies all buffers contained 15 mM HEPES (final pH 7.4). Valinomycin (10 μ M) was present in the DNP treatment (*i. e.*, preloading) buffer. When an inside negative potential was created, DNP treatment buffers contained 40 mM KCl and uptake was carried out in

K⁺-free buffer with 40 mM mannitol. In the voltage clamped condition, preloading and uptake buffers contained equal concentration of KCl (*i. e.*, 40 mM). When a Na⁺ gradient was tested, preloading buffers contained choline chloride (100 mM) and uptake mixtures contained NaCl (100 mM). When taurine uptake in equal Na⁺ or no Na⁺ was tested, equal concentrations of either NaCl (100 mM) or choline chloride (100 mM) was present in both preloading and uptake buffers.

Uptake Studies

The uptake of taurine into the choroid plexus was examined by incubating the tissue slices at 37°C with 140 μ l of uptake mixture that contained [³H] taurine (0.0391 μ M), [¹⁴C] mannitol (17.9 μ M) and unlabeled taurine (25 μ M) in an appropriate buffer (see figure legends). DNP (250 μ M) was present to ensure continued depletion of ATP. Under the voltage clamped condition, Na⁺-dependent taurine uptake was linear and reproducible at 15 minutes (Fig. 2). Therefore, uptake at 15 minutes was determined in subsequent studies.

For inhibition studies, the uptake (at 15 min) was studied in the presence of [³H]-taurine and test compounds (2 mM). For all studies, uptake was terminated by removing the tissue from the uptake mixture and blotting it on laboratory tissue paper. The blotted tissue was placed on a pre-weighed piece of aluminum foil, dried under an IR-lamp heater for 1 hr, and then weighed to calculate the net dried tissue weight. The tissue was carefully detached from the foil with a forceps and digested in 50 μ l of 3 N KOH solution in a liquid scintillation counting vial. After the tissue was completely dissolved, the identical volume of 3 N HCl solution was added to neutralize the KOH. After the corresponding aluminum foil piece was added to the vial, the tissue associated radioactivity was determined by liquid scintillation counting. In addition, the uptake mixture (50 μ l) was sampled and added to separate vials

for liquid scintillation counting. [^{14}C] and [^3H] were determined by a dual isotope liquid scintillation counting on a Beckmann Model 1801 liquid scintillation counter (Beckmann Instruments Inc., Fullerton, CA). Counting efficiency of [^3H] ranged from 45 to 47% and of [^{14}C] ranged 92 to 94%.

Stereotaxic Surgery

Rats underwent a stereotaxic surgery to implant cannulae into the lateral ventricle and the cisterna magna.²⁰ Briefly, the rat was mounted on a stereotaxic device (David Kopf Instrument, Tujunga, CA) under a ketamine and acepromazine anesthesia (80 mg/kg and 10 mg/kg, respectively). The frontal, parietal and occipital bones were exposed through a linear midline incision. Using coordinate obtained from a stereotaxic atlas of rat brain,²¹ the left lateral ventricle was located (1.0 mm posterior, 1.6 mm lateral, and 3.6 mm ventral to the bregma). A burr hole was drilled and a steel guide cannulae (22GA, 4 mm below the pedestal, Plastics One, Roanoke, VA) was lowered using an electrode manipulator of the stereotaxic device to pierce the dura and enter the lateral ventricle. The cannulae was secured to two anchoring screws using a dental acrylic cement (Lang Dental, Chicago, IL).

A polyethylene catheter was also placed into the cisterna magna for serial sampling of the CSF. The catheter consisted of PE10 (9.5 mm in length) tubing, inserted 3 mm inside PE 50 tubing (20 mm in length). A stainless steel wire was inserted inside the PE tubings to add rigidity to facilitate piecing the dura. A burr hole was drilled at 3 mm posterior to the lambda and the PE 10 portion of the catheter was inserted caudally. The stainless steel guide was then removed. A microsyringe (Gastight #1802, Hamilton Co., Reno, NV) was connected to the catheter and CSF flow was induced by a gentle pull of the syringe. Upon confirming the CSF flow, the microsyringe was disconnected and the catheter was secured to two anchoring screws by a dental acrylic. The animal

was allowed to recover for 1.5 hr before the start of the study. The ketamine/acepromazine anesthesia was maintained throughout the study.

Ventriculocisternal Procedure

The objectivity of this study was to determine elimination kinetics of taurine from the rat CSF. Thus, 5 μl of solution, containing ^3H -taurine (40 pmole) and ^{14}C -mannitol (60 μg ; *i.e.*, a marker of the CSF flow) in sterile water, was administered into the lateral ventricular cannulae using a microsyringe (Hamilton Co., Reno, NV). Sterile water was used as a vehicle because mock CSF or physiological saline would have produced a hypertonic injection solution (*i.e.*, approximately 700 mOsm). Preliminary experiments showed that taurine elimination kinetic was not significantly affected by vehicles (data not shown).

Taurine dose dependency was studied, 0.3 μmole or 2 μmole of unlabelled taurine was administered along with the radio-labelled compounds. When selectivity of taurine elimination was studied, 2 μmole of α - or β -alanine was added to the injection solution. The CSF sample (5 μl) was collected at time 2, 5, 15, 30, 45, 60, 90, 120, 180 min. Scintillation fluid (5 ml) was mixed with the CSF and the radioactivity in the CSF was then determined by a dual isotope liquid scintillation counting.

The distribution of ^3H -taurine into selected parts of brain was determined at the end of the 180 min CSF collection. The rat was decapitated and the brain was immediately removed. Representative samples (approximately 10 mg) from the olfactory bulb, cortex and cerebellum were obtained. Also, the choroid plexi from each lateral ventricle were obtained. The dissection and the isolation procedure was completed in approximately 10 min. Isolated brain tissues were then weighed on pre-weighed aluminum foils and dissolved in 200 μl of 3N NaOH overnight. After the tissue was completely dissolved, 50 μl aliquots of tissue lysate were added to scintillation vial.

Then, the lysate was neutralized with 50 μ l of 3N HCl solution and the tissue associated radioactivity was determined by a dual isotope liquidscintillation counting. Tissue to media (T/M) ratio, representing the distribution of radiolabelled taurine into the representative brain tissue, was then calculated.

Pharmacokinetic Analysis

Kinetics of taurine disappearance from the CSF were analyzed by a standard pharmacokinetic analysis. A potential pharmacokinetic model was first constructed by assuming first order elimination from the CSF via bulk flow clearance, saturable distribution into the brain tissue, including the choroid plexus, and first order transfer from the deep to the shallow compartment. In this model, we assumed that the saturable rate process is reasonably described by the Michaelis-Menten kinetics. Then, the mass balance was written as shown in Scheme 1, model 1. Definition of pharmacokinetic variable is as follows: V_1 , the apparent volume of distribution of the CSF; CL_{bulk} , bulk flow clearance; CL_{21} , transfer clearance from the brain tissue to the CSF; V_{max} , apparent maximal velocity; K_M , the Michaelis-Menten constant; V_2 , apparent volume of distribution of the brain tissue. Then, more complex pharmacokinetic models were built on to model 1 (e.g., an additional saturable elimination from the CSF was added in model 2; see Scheme 1). Overall, four potential pharmacokinetic models were constructed and analyzed to determine the model which best describes our results with the least complexity.

Since the equations in Scheme 1 contained non-linear terms, C_{CSF} cannot be analytically integrated to obtain a concentration vs. time relationship. Therefore, all the data in the taurine dose dependency study were simultaneously fitted to each model by the Runge-Kutta numerical integration method using PCNONLIN (Statistical Consultants Inc., Lexington, KY) running on a 386 personal computer. The sums of squares, the

Akicke's information criteria, and the Schwartz criteria were then calculated to determine the most appropriate pharmacokinetic model.

Data Analysis

The uptake of taurine into the choroid plexus was expressed as volume of distribution (V_d),¹⁹ which is essentially a concentration ratio of tissue to media, by the following equation:

$$V_d = \frac{\text{dpm}[^3\text{H}] \text{ taurine in choroid plexus/g of choroid plexus}}{\text{dpm}[^3\text{H}] \text{ taurine in media/ml of media}}$$

$$\frac{\text{dpm}[^{14}\text{C}] \text{ mannitol in choroid plexus/g of choroid plexus}}{\text{dpm}[^{14}\text{C}] \text{ mannitol in media/ml of media}}$$

When taurine uptake into the brain tissue of the rat was examined, a tissue to media ratio (T/M)¹⁹ was calculated by the following equation:

$$T/M = \frac{\text{dpm}[^3\text{H}] \text{ taurine in brain tissue/g of brain tissue}}{\text{dpm}[^3\text{H}] \text{ taurine in CSF at 3 hr/ml of CSF}}$$

$$\frac{\text{dpm}[^{14}\text{C}] \text{ inulin in brain tissue/g of brain tissue}}{\text{dpm}[^{14}\text{C}] \text{ inulin in CSF at 3 hr/ml of CSF}}$$

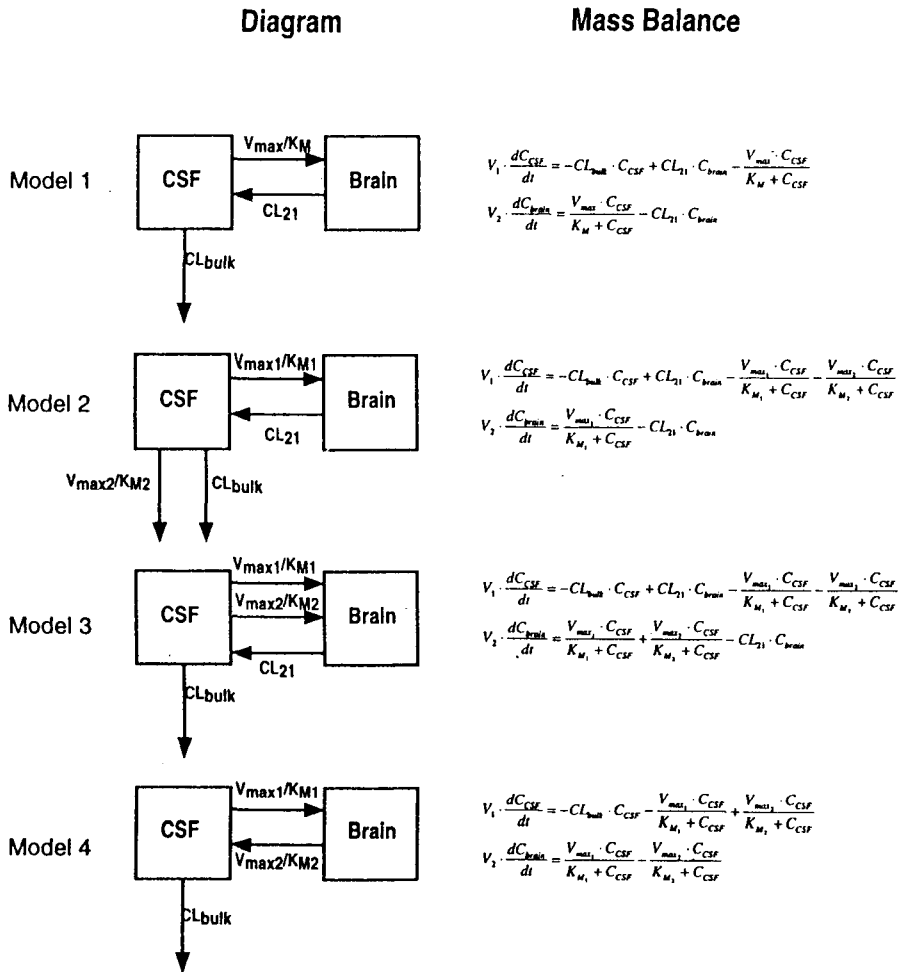
For the Michaelis-Menten studies, the initial rate of uptake was expressed as nmoles/g of choroid plexus/15 min and plotted against the initial concentration of taurine. The data were fit to the following equation:

$$\text{Rate} = \frac{V_{max} \cdot C_{\text{taurine in uptake mixture}}}{K_M + C_{\text{taurine in uptake mixture}}}$$

where V_{max} is the maximal uptake rate and K_M is the concentration of taurine when the rate is 50% of the maximal rate. The data were fit to this equation using a non-linear regression program on Kalidagraph® (version 2.0, Synergy Software, Reading, PA) on a Macintosh SE computer.

To determine the stoichiometric coupling ratio of Na^+ and taurine, the Hill equation was used:

$$\text{Rate} = \frac{V_{max} \cdot C_{\text{Na}^+ \text{+ taurine in uptake mixture}}^n}{K_M^n + C_{\text{Na}^+ \text{+ taurine in uptake mixture}}^n}$$



Scheme I.

where V_{max} is the initial rate at the saturating concentration of Na^+ , K_M is the concentration of Na^+ at half maximal rate, and n is Hill's coefficient.²²⁾ However, since we could not achieve the saturating concentration of Na^+ in the physiological osmolarity range (*i.e.*, up to 250 milliosmolar), the data were fit to a simplified version of Hill's equation :

$$Rate = a \cdot C_{Na+in\ uptake\ mixture}^n$$

where a is essentially V_{max} / K_M^n when $K_M^n \gg C_{Na+in\ uptake\ mixture}^n$. The data were transformed with a logarithm and linearly regressed to obtain a and n .

To calculate the apparent clearance and the volume of distribution, the moment analysis was used.²³⁾ The areas under the concentration vs. time curve (AUC) and the concentration-time product vs. time curve (AUMC) were calculated by a linear trapezoidal method up to 180 min. Remaining area to infinity for AUC was then estimated by dividing concentration of the last collection time by the terminal slope. Remaining area from the last sampling time to infinity for AUMC was estimated by the following equation :

$$\int_{3\ hr}^{\infty} C_{CSF} dt = \frac{(t \cdot C_{CSF})_{3\ hr}}{\text{terminal slope}} + \frac{C_{CSF, 3\ hr}}{\text{terminal slope}^2}$$

The apparent clearance was then calculated by dividing dose by AUC. The volume of distribution (V_{ss}) was calculated by the following equation :

$$V_{ss} = \frac{\text{Dose} \cdot \text{AUMC}}{\text{AUC}^2}$$

In general, each data point was determined in triplicate and a minimum of 3 experiments was carried out. Data are expressed in terms of mean \pm standard deviation (S.D.) of all determinations. Means were compared using unpaired Student's t-test or one-way ANOVA and $p < 0.05$ was accepted as denoting statistical significance.

Results

Time Course of Taurine Uptake

The uptake of taurine into ATP-depleted choroid plexus slices was examined in the presence and absence of an inwardly directed Na^+ gradient (120 mM) (Fig. 1). The uptake of taurine was significantly greater ($p < 0.001$, except at 2 min) in the presence of a Na^+ gradient, compared to the uptake when Na^+ was present at equal concentrations inside and outside the tissue slices. Also, in the absence of Na^+ (*i.e.*, equal K^+ concentration inside and outside), the accumulation was depressed further than that in the presence of equal Na^+ concentration ($p < 0.01$, except 2 and 90 min).

In the presence of an inwardly directed Na^+ gradient, the accumulation of taurine into the tissue reached a maximum at approximately 15 min (5.76 ± 0.619 ml/g), after which the concentration of taurine in the tissue declined with time (at 3 hrs 3.12 ± 0.356 ml/g, $p < 0.001$ compared to Vd at 15 min). Although a distinct "overshoot phenomenon" was not observed, taurine accumulation in the presence of an initial Na^+ gradient was still statistically greater at 3 hours than that obtained when the Na^+ concentration was equal inside and outside ($p < 0.001$), suggesting that an equilibrium was not achieved.

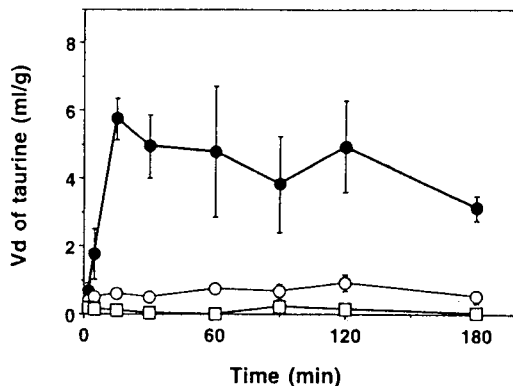


Figure 1—Temporal profile of taurine accumulation in ATP-depleted rabbit choroid plexus. Uptake (in Vd) of taurine (25 μM) was determined at 37°C. Points represent the mean \pm S.D. of data from 5 experiments. Each experiment consisted of triplicate measurements of uptake.

Key : ●; 120 mM inwardly directed Na^+ gradient, ○; 120 mM equal Na^+ inside and outside of the tissue, □; 120 mM equal K^+ inside and outside of the tissue.

Electrogenicity Studies

To determine whether the Na^+ -driven transport of taurine in the choroid plexus is electrogenic, we studied Na^+ -driven taurine uptake in the presence and absence of an electrical potential difference. (Fig. 2). At 1, 5 and 15 min, taurine uptake in the ATP-depleted choroid plexus was enhanced when an inside negative electrical potential gradient was created ($p < 0.05$), suggesting that Na^+ -dependent taurine uptake is electrogenic. However, the enhanced accumulation of taurine was no longer apparent at 60 min, most likely because the potential difference had dissipated. Electrical potential alone, however, could not drive taurine accumulation (Fig. 2). Since choline and valinomycin may have affected taurine uptake in ATP-depleted choroid plexus, control studies were performed to test the effects of these compounds. Neither choline nor valinomycin directly affected Na^+ -driven taurine uptake (data not shown).

Concentration-dependency and Stoichiometry Studies

The rate of taurine uptake as a function of co-

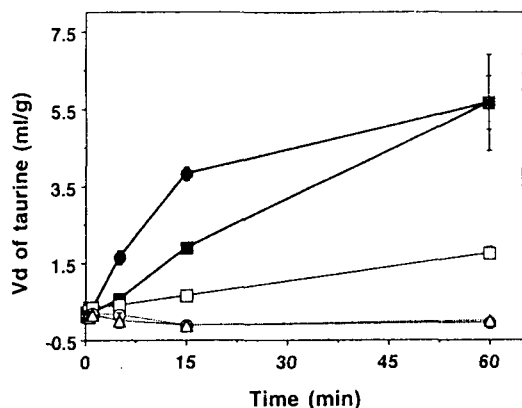


Figure 2—Effect of potential gradient and Na^+ gradient on the uptake of taurine ($25 \mu\text{M}$) in ATP-depleted rabbit choroid plexus. Data represent the mean \pm S.D. of 3 experiments. Each experiment consisted of triplicate measurements of uptake.

Key: ●; 100 mM inwardly directed Na^+ -gradient in addition to inside negative potential gradient, ■; 100 mM inwardly directed Na^+ gradient under voltage clamp condition, ○; 100 mM equal Na^+ concentration inside and outside of tissue with inside negative potential gradient, △; 100 mM equal choline⁺ concentration inside and outside of tissue with inside negative potential gradient ○; 100 mM equal choline⁺ concentration inside and outside of tissue under voltage clamp condition.

concentration was determined at 15 min in the presence of an inwardly directed Na^+ gradient under voltage clamped conditions (Fig. 3). The uptake rate of taurine was saturable, consistent with the Michaelis-Menten kinetics. The data were fit to equations involving one as well as two Michaelis-Menten terms. However, the goodness of the fit was not significantly improved in the more complex kinetic model. Therefore, the simpler kinetic model with a single saturable component was selected. The estimated V_{max} and K_M were $111 \pm 20.2 \text{ nmol/g/15 min}$ and $99.8 \pm 29.9 \mu\text{M}$, respectively. We did not correct for the non-saturable component of taurine uptake, since the uptake values for the four highest concentrations of taurine were not statistically different, indicating that nonsaturable taurine uptake is not a major component of the overall taurine transport

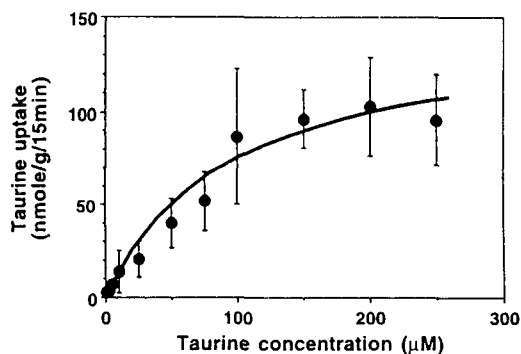


Figure 3—Concentration dependency of taurine uptake. Uptake in nmole/g/15 min was measured at 37°C . This study was carried out in the presence of inwardly directed 120 mM Na^+ gradient under voltage clamped conditions. Points represent the mean \pm S.D. of data from 3 experiments. Each experiment consisted of triplicate measurements of uptake. Taurine uptakes for 4 highest substrate concentrations were not statistically different from each other (one-way ANOVA).

into the tissue.

To assess the stoichiometry of the Na^+ -dependent taurine transport, the effect of various concentrations of Na^+ (5 to 120 mM) on the uptake of taurine ($25 \mu\text{M}$) at 15 min was examined (Fig. 4). The uptake of taurine was dependent on the Na^+ concentration. The estimated slope coefficient, n , was 1.80 ± 0.122 (mean \pm standard error), consistent with a 2:1 Na^+ : taurine ratio.

Inhibition Studies

The effect of various potential inhibitors of taurine transport in choroid plexus was examined (Table I). At a concentration of 2 mM, the α -amino acids, L-alanine, glycine and glutamate, did not affect taurine uptake. However, β -amino acids (*i.e.*, β -alanine, taurine and hypotaurine) inhibited taurine uptake significantly ($p < 0.05$), indicating that the Na^+ -driven taurine transporter in the choroid plexus is selective for β -amino acids.

Taurine Dose-Dependency Study

When 40 pmole of radiolabelled taurine was injected into the lateral ventricle, the concentra-

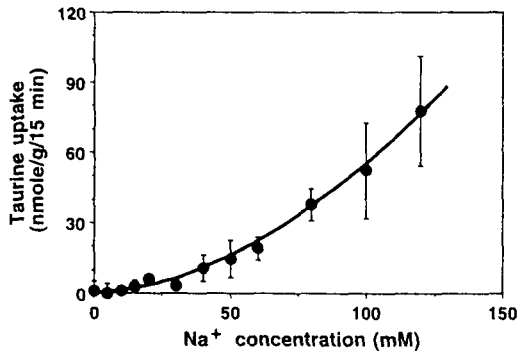


Figure 4—Effect of Na⁺ concentration on taurine uptake. Uptake of taurine (25 mM) in nmole/g/15 min was measured at 37°C under voltage clamped condition. Points represent the mean \pm S.D. of data from 3 experiments. Each experiment consisted of triplicate measurements of uptake. Observed Vd value for taurine is represented by solid circle. The computer generated fit, estimated by the modified Hill's equation (see Material and Method section), is shown by a solid line.

Table I—The Uptake of Taurine (25 μ M) in the Presence of Potential Inhibitors. Data were Obtained from 3 Experiments. Each Experiment Consisted of Triplicate Measurements of Uptake. Unless Specified, Values Represent Taurine Uptake (Vd) with a 120 mM Inwardly Directed Na⁺ Gradient in the Presence of Various Inhibitors at 15 min at 37°C.

Test condition	Vd of taurine (ml/g)		% of control	p value
	mean	S. P.		
Control, taurine 25 μ M	4.85	0.675	100	-
no Na ⁺ gradient	0.487	0.189	10.0	p<0.01
Taurine, 2 mM	1.98	0.554	40.9	p<0.05
Hypotaurine, 2 mM	0.593	0.296	12.2	p<0.01
β -Alanine, 2 mM	0.838	0.510	17.3	p<0.01
L-alanine, 2 mM	5.05	1.18	104	N.S. ^a
Glycine, 2 mM	4.35	1.26	89.7	N.S. ^a
Glutamate, 2 mM	4.41	0.776	90.9	N.S. ^a

^a N.S.: not significant

^{*} p value by t-test compared to control.

tion of taurine declined in a bi-exponential manner (Fig. 5) while inulin followed an apparent mono-exponential decline (data not shown). The clearances, calculated from the moment parameter, for taurine (40 pmole) and inulin were 73.4

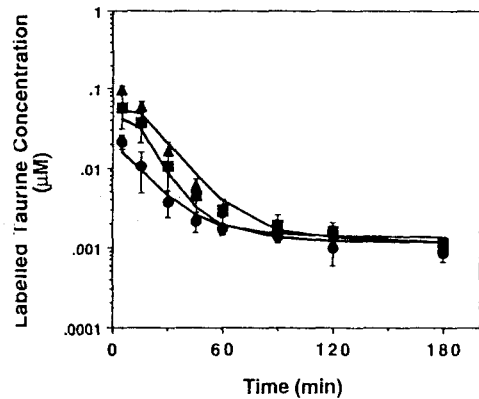


Figure 5—Dose dependency of radiolabelled taurine concentration in the CSF vs. time curve.

Key: ●, 40 pmole labelled taurine dose; ▲, 40 pmole labelled taurine + 0.3 μ mole unlabelled taurine dose; ■, 40 pmole labelled taurine + 2 μ mole unlabelled taurine dose. Solid line was generated by a nonlinear regression fitting of a pharmacokinetic model shown in Scheme 1, model 1 with parameters in Table IV. Data are expressed as means of 3 runs \pm S.D.

$\pm 27.7 \mu$ /min and $3.85 \pm 1.08 \mu$ /min, respectively ($p < 0.005$). When 40 pmole of the labelled taurine was administered with 0.3 μ mole of unlabelled taurine, the apparent clearance for the labelled taurine was decreased to $24.7 \pm 11.8 \mu$ /min ($p < 0.01$). The clearance was further decreased in the presence of 2 μ mole of unlabelled taurine ($15.5 \pm 0.0438 \mu$ /min). This observation suggests that taurine disappeared from the CSF by a clearance process(es) in addition to bulk flow and that the additional clearance process is saturable. The decrease in the clearance was associated with similar decrease in the V_{ss} parameter ($p < 0.01$, Table II). The inulin clearance was not affected by the unlabelled taurine co-administration.

The uptake of labelled taurine was also examined in representative brain areas. When expressed as a tissue to media ratio (T/M, in ml/g) at 3 hrs, taurine uptake into the choroid plexus was at least 10 fold higher than in other parts of the brain (Fig. 6, $p < 0.005$). In addition, taurine uptake into the cortex and the choroid plexus

decreased in a dose-dependent manner ($p < 0.01$, Fig. 6). These observations suggest that the saturable disposition of taurine in the CSF is due to saturable distribution of taurine into the brain.

Pharmacokinetic Analysis

To analyze these observations quantitatively, four potential pharmacokinetic models were constructed (Scheme 1) and a nonlinear regression analysis was conducted via a simultaneous fitting of all three dose (8 observations for each dose, Fig. 5) to each pharmacokinetic model shown in Scheme 1. Therefore, this analysis would allow an estimation of pharmacokinetic parameters encompassing a dose range of 62,500 fold. The Akaike's information criteria and the Schwarz criteria were calculated to determine a model which best describes our results with the least complexity (Table III). Also, weighted sums of squares was calculated to select a model that results in the least deviation from the observations. Based on all the criteria we used, model 1 best described our results (Table IV)

Discussion

Taurine is highly concentrated in the mamma-

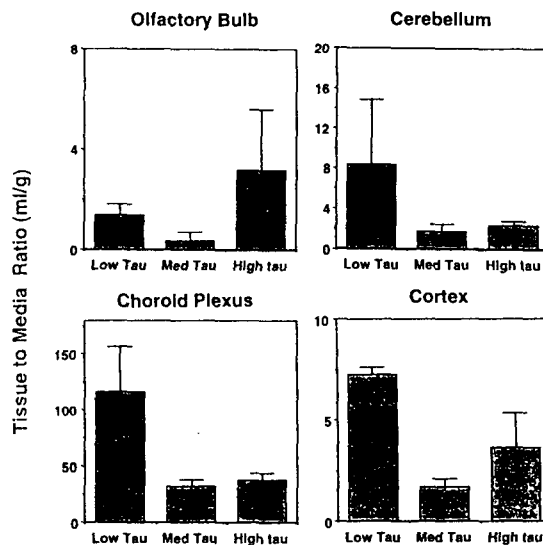


Figure 6—Distribution of radiolabelled taurine in brain areas 3 hr after administration.

Key: Low TAU, 40 pmole labelled taurine dose; Med TAU, 40 pmole labelled taurine + 0.3 μ mole unlabelled taurine dose; High TAU, 40 pmole labelled taurine + 2 μ mole unlabelled taurine dose; Panel A, taurine distribution in the olfactory bulb; Panel B, taurine distribution in the choroid plexus; Panel C, taurine distribution in the cerebellum; Panel D, taurine distribution in the cortex. Data are expressed as means of 3 runs \pm S.D. *: statistically different from Low TAU by $p < 0.05$ (t-test). **: statistically different from Low Tau by $p < 0.01$ (one-way ANOVA, followed by Turkey's multiple comparison test).

Table II—Clearance and Volume of Distribution of Taurine and Inulin in Dose Dependency and in Inhibitor Studies. The Zero (i.e., Area Under the Taurine Concentration in the CSF vs. Time) and the First (i.e., Area Under the Product of Time and the Concentration vs. Time) Moments were Calculated by the Linear Trapezoidal Rule. Apparent Clearance and Volume of Distribution were then Calculated by the Standard Pharmacokinetic Method. Data are Expressed in the Means \pm S.D. of Three Runs.

	Taurine		Inulin	
	Apparent Clearance (μ /min)	Vss(ml)	Apparent Clearance(μ /min)	Vd(ml)
Low taurine dose (40 pmole taurine)	73.4 \pm 27.7	5.23 \pm 2.26	3.85 \pm 1.08	0.240 \pm 0.106
Medium taurine dose (0.3 μ ole taurine)	24.7 \pm 11.8**	1.56 \pm 1.22**	5.04 \pm 1.64	0.253 \pm 0.082
High taurine dose (2 μ ole taurine)	15.5 \pm 0.0437**	0.819 \pm 0.161**	7.34 \pm 3.36	0.404 \pm 0.178
β -alanine coadministration (40 pmole taurine + 2 μ ole β -alanine)	8.85 \pm 1.29*	0.414 \pm 0.225*	3.97 \pm 0.659	0.2047 \pm 0.0528
α -alanine coadministration (40 pmole taurine \pm 2 μ ole α -alanine)	12.5 \pm 1.15*	0.430 \pm 0.245*	3.44 \pm 0.409	0.162 \pm 0.0384

*; statistically different from low taurine dose by $p < 0.05$ (t-test)

**; statistically different from low taurine dose by $p < 0.01$ (one-way ANOVA and Turkey's multiple comparison)

Table III—Summary of Non-linear Regression Analysis.

	AIC ^a	SC ^b	Sum of residual
Model 1	33.9	43.4	2.11
Model 2	84.1	93.6	17.1
Model 3	50.9	60.3	4.28
Model 4	N.A. ^d	N.A.	N.A.

^a: Akaike's Information Criteriaon (AIC)= $N \cdot \ln(\text{Sum of residual}) + 2 \cdot p$ where N represents number of observations and p is number of parameters in a model

^b: Schwartz Criteria (SC)= $N \cdot \ln(\text{Sum of residual}) + p \cdot \ln(N)$

^c: Sum of residual $\sum_{i=1}^N \{(y_{i, obs} - y_{i, cal})^2 / y_{i, obs}\}$

where $y_{i, obs}$ represents observed concentration and $y_{i, cal}$ is calculated concentration based on a pharmacokinetic model

^d: N.A., not applicable. A convergence could not be achieved for this pharmacokinetic model and, therefore, AIC, SC and sum of residual could not be calculated.

Table IV—Summary of Estimated Pharmacokinetic Parameters. Pharmacokinetic Parameters were Estimated Based on Model 1 (Scheme1). Data from Taurine Dose Dependency Study was Used in the Non-linear Regression Analysis. The Estimates are Represented by Estimated Parameter \pm Standard Error Generated during the Fitting Procedure.

Pharmacokinetic parameters	Regression estimate
V_1 (ml)	0.21 \pm 0.051
V_{max} (nmole/min)	4.1 \pm 2.2
K_M (μ M)	40 \pm 25
V_2 (ml)	56 \pm 35
CL_{21} (ml/min)	0.17 \pm 0.12
CL_{bulk} (ml/min)	0.026 \pm 0.0059

lian brain and is known to have important functions in the CNS.¹⁻⁶ In particular, it has been suggested that taurine is vital for the normal development of the brain, and deficiency is associated with neurologic dysfunction.¹⁻³ For example, pediatric patients who develop taurine deficiency while receiving long term intravenous alimentation have abnormal electroretinograms.²³

Taurine is a polar molecule, and therefore its movement across biological membranes must in-

volve interaction with transport system(s), since simple diffusion should be insignificant. Indeed, Na^+ -driven taurine transport has been identified in a variety of tissues.²⁴⁻²⁶ However, the specific transport systems at the barriers between the systemic circulation and the brain have not been studied extensively. The physiological significance of such transport mechanism is further emphasized by the fact that taurine homeostasis in the brain appears to be tightly regulated.^{27, 28} This regulation may occur at a site of a concentrative transport system which mediates taurine's entry into and/or exit from the extracellular fluid of the brain.

In this study, we demonstrated that a specific Na^+ -driven system for the transport of β -amino acids exists in the choroid plexus of the rabbit.

By ATP-depleting the tissue, it was possible to test the role of ion gradients in the transport of a particular substrate.^{17, 19} In the presence of an initial inwardly directed Na^+ gradient, taurine uptake was greatly enhanced. However, only a slight overshoot phenomenon, characteristic of a concentrative uptake, was achieved. This pattern of transport is consistent with an extremely slow efflux of taurine from the tissue. In this study, we did not investigate the mechanisms of taurine efflux in the choroid plexus tissue slices. However, the efflux half-life of taurine from different areas of rat brain ranges from 9 to 240 hours,²⁹ supporting the speculation that taurine exits slowly from choroid plexus tissue.

We examined the Na^+ -taurine coupling ratio by controlling the Na^+ -gradient in the ATP-depleted tissue. The data are consistent with coupling ratio of 2:1 for Na^+ -dependent taurine transport. Similar coupling ratios have been reported in renal²⁵ and placental²⁴ brush border membrane vesicles. However, maximal velocity of taurine transport was not achieved even in the presence of a Na^+ concentration of 120 mM. Similarly, maximal taurine transport was not clearly reached at a Na^+

concentration of 200 mM in renal brush border membrane vesicles.²⁵⁾ We did not examine taurine uptake in the presence of a higher Na^+ -gradient, since extending the Na^+ concentration beyond 120 mM may not be physiologically relevant and hyperosmotic conditions are known to increase taurine uptake in a number of tissues.³⁰⁻³²⁾

The stoichiometry data are consistent with the finding that a transient inside-negative potential difference could enhance the uptake of taurine in the ATP-depleted choroid plexus (Fig. 2). That is, with a coupling ratio of 2:1, the inward transport of the electrically neutral taurine results in a net uptake of positive charges (*i.e.*, Na^+).

The Na^+ -dependent taurine uptake into the ATP-depleted choroid plexus slices was saturable, consistent with the Michaelis-Menten kinetics. The estimated K_M was 99.8 μM , suggesting a high affinity transport system, and is slightly higher than K_M values reported in other tissues (*i.e.*, 4-86 μM).²⁴⁻²⁷⁾ The selectivity of the transport in rabbit choroid plexus also exhibited a similar pattern to that reported in other tissues and species. Only β -alanine and hypotaurine inhibited taurine uptake, while the α -amino acids did not affect taurine transport (Table II). Therefore, the taurine transporter we characterize in this study appears to be consistent with the previously described system β -amino acid transporter.^{33,34)} Interestingly, a high concentration of unlabeled taurine (2 mM) did not completely inhibit taurine uptake, suggesting that there may be a low affinity taurine uptake system in the choroid plexus.

In this study, we demonstrated that taurine is eliminated from the CSF by a mechanism in addition to bulk flow and that this additional clearance process decreased with taurine dose (Table II). The decrease in the clearance of taurine was accompanied by a similar decrease in the volume of distribution (Table II) and in the distribution of taurine into specific brain areas (Fig. 6). These observations indicate that the distribution of tau-

rine into the brain is saturable. Therefore, a standard pharmacokinetic analysis was performed to estimate distribution and elimination kinetics of taurine. Nonlinear regression analysis revealed that the taurine distribution into the brain compartment was saturable with estimated K_M of 40 μM . Also, estimated volume of distribution for the brain compartment is 56 ml, indicating the taurine readily distributed into the brain. This estimation is consistent with a high concentration of taurine in the brain. The volume of taurine distribution into the CSF compartment was estimated to be 0.210 ml, similar to the estimated volume of CSF (*i.e.*, inulin volume of distribution, Table II). As expected, first order clearance of taurine from the CSF was estimated to be 26 $\mu\text{l}/\text{min}$, close to the apparent clearance in medium and high taurine dose (Table II). Overall, the goodness of the fit acceptable considering the dose range of 62,500 fold (Fig. 5).

Taurine distribution into the representative brain areas was dose-dependent (Fig. 6). Among the brain areas examined, the choroid plexus had at least 10 fold higher tissue to media ratio for all doses. In addition, the calculated tissue to media ratio at 3 h for the choroid plexus was over 100, indicating the taurine concentration in the choroid plexus was substantially higher than that of the CSF. In this study, we did not attempt to characterize the release kinetics of taurine into the systemic circulation from the choroid plexus. However, in a preliminary experiment, we attempted to measure the concentration of radio-labelled taurine in the systemic circulation after taurine was administered into the lateral ventricle. We could not detect any radioactivity in the plasma up to 2 hr after the injection (data not shown), a time when the taurine in the CSF would have reached an equilibrium with the choroid plexus. Taken together, these observations suggest that taurine is actively transported into the choroid plexus, and leaks out from the tissue

slowly. Such slow release of taurine from variety of tissue has been reported in both *in vivo* and *in vitro* studies.²⁹

The Michaelis-Menten rate constant obtained *in vivo* taurine dose dependency study was similar to that found in the uptake experiment. These data are consistent with the hypothesis that high affinity, Na⁺-dependent transport plays a role, at least in part, in taurine elimination from the CSF, indicating that the Na⁺-dependent taurine transporter is responsible for the small CSF to plasma concentration ratio for taurine. However, further studies (*e.g.*, *in situ* hybridization study) will be necessary to elucidate clearly the location of the transporter and its physiologic significance. In conclusion, we have characterized the Na⁺-dependent taurine uptake in ATP-depleted rabbit choroid plexus. The process appears electrogenic with an estimated coupling ratio of 2 Na⁺ to 1 taurine molecule. The accumulation of taurine is saturable with high selectivity for β -amino acids. This uptake system may be functionally relevant in maintaining taurine homeostasis in CSF and, ultimately, the extracellular fluids of the brain.

References

- 1) Sturman J.A., Gargano A.D., Messing J.M. and Imaki H., *J. Nutr.* **116**, 655-677(1986).
- 2) Sturman J.A., Moretz R.C., French J.H. and Wisniewski H.M., *J. Neurosci. Res.* **13**, 405-416(1985).
- 3) Palackal T., Moretz R.C., Wisniewski H.M. and Sturman, J. *Brain Dysfunc.* **1**, 71-89(1988).
- 4) Palackal T., Moretz R., Wisniewski H. and Sturman J.A., *J. Neurosci. Res.* **15**, 223-239 (1986).
- 5) Kuriyama K., *Fed. Proc.* **39**, 2680-2684(1980).
- 6) Huxtable R.J., *Prog. Neurobiol.* **32**, 471-533 (1989).
- 7) Lefauconnier J.M., Urban F. and Mandel P., *Biochim.* **60**, 381-387(1978).
- 8) Jhiang S.M., Fithian L., Smanik P., McGill J., Tong, Q. and Maxxaderri E.L., *Febs. Lett.* **318**, 129-144(1993).
- 9) Ramamoorthy S., Leibach F.H., Mahesh V.B., Han H., Yang-Feng T., Blakely R.D. and Ganapathy V., *Biochem. J.* **300**, 893-900(1994).
- 10) Liu Q.R., Lopez-Corcuera B., Nelson H., Mandiyan S. and Nelson N., *Proc. Natl. Acad. Sci.* **89**, 12145-12149(1992).
- 11) Caruthers J.S. and Lorenzo A.V., *Brain Res.* **73**, 35-50(1974).
- 12) Snodgrass S.R., Cutler R.W.P., Kang E.S. and Lorenzo A.V., *Am. J. Physiol.* **217**, 974-980 (1969).
- 13) Preston J.E. and Segal M.B., *Brain Res.* **525**, 275-279(1990).
- 14) Segal M.B., Preston J.E., Collis C.S. and Zlokovik B.V., *Am. J. Physiol.* **258**, 1288-1294 (1990).
- 15) Perry T.L., Hansen S. and Kennedy J., *J. Neurochem.* **24**, 587-589(1975).
- 16) McGale E.H.F., Pye I.F., Stonier C., Hutchinson E.C. and Aber G.M., *J. Neurochem.* **29**, 291-297(1977).
- 17) Carter-Su C. and Kimmich G.A., *Am. J. Physiol.* **237**, 64-74(1979).
- 18) Suzuki H., Sawada Y., Sugiyama Y., Iga T. and Hanano M., *J. Pharmacol. Exp. Ther.* **243**, 1147-1152(1987).
- 19) Wu X., Yuan G., Brett C.M., Hui A.C. and Giacomini K.M., *J. Biol. Chem.* **267**, 8813-8818(1992).
- 20) Wu X., Hui A.C. and Giacomini, K.M., *Pharmaceut. Res.* **10**, 611-615(1993).
- 21) Paxinos G. and Watson, C., *The rat brain in stereotaxic coordinates*, 2nd ed., Academic Press, New York(1986).
- 22) Segal I.H., *Enzyme Kinetics*, pp. 398-404, John Wiley & Sons Inc., New York(1975).
- 23) Gibaldi, M and Perrier, D., *Pharmacokinetics*, 2nd Ed., pp. 409-417, Marcel Dekker, New York(1982).
- 24) Geggel H.S., Ament M.E., Heckenlively J.R., Martin D.A. and Kopple J.D., *N. Engl. J. Med.* **312**, 142-146(1985).
- 25) Moyer M.S., Insler N. and Dumaswala R., *Biochim. Biophys. Acta.* **1109**, 74-80(1992).

- 26) Jessen H. and Sheikh M.I., *Biochim. Biophys. Acta.* **1064**, 189-198(1991).
- 27) Trachtman H., Futterweit S. and Sturman J. A., *Diabetes* **41**, 1130-1140(1992).
- 28) Chesney R.W., Gusowski N., Lippincott S. and Zelikovic I., *Pedi. Nephrol.* **2**, 146-150(1988).
- 29) Chesney R.W., Zelikovic I., Dabbagh S., Friedman A. and Lippincott S., *J. Exp. Zoo.* **248**, 25-32(1988).
- 30) Collins G.G.S., *Brain Res.* **76**, 447-459(1974).
- 31) Uchida S., Nakanishi T., Kwon H.M., Preston A.S. and Handler J.S., *J. Clin. Invest.* **88**, 656-662(1991).
- 32) Lien Y.H.H., Shapiro J.I. and Chan L., *J. Clin. Invest.* **85**, 1427-1435(1990).